M. ŻELECHOWER*, J. KLIŚ**, E. AUGUSTYN*, J. GRZONKA***, D. STRÓŻ****, T. RZYCHOŃ*, H. WOŹNICA*

## THE MICROSTRUCTURE OF ANNEALED *GALFAN* COATING ON STEEL SUBSTRATE

## MIKROSTRUKTURA WYGRZEWANYCH POKRYĆ CYNKOWYCH TYPU *GALFAN* NA PODŁOŻU STALOWYM

The commercially available *Galfan* coating containing 5-7wt.% of Al deposited on the low carbon steel substrate by hot dipping has been examined with respect to the microstructure of the coating/substrate interface area. The application of several experimental techniques (SEM/EDS, XRD, TEM/AEM/EDS/ED) allowed demonstrating the two-phase structure of the alloy coating in non-treated, commercially available *Galfan* samples: Zn-rich pre-eutectoid $\eta$ phase grains are surrounded by lamellar eutectics of $\beta$-Al and $\eta$-Zn. The transition layer between the alloy coating and steel substrate with the considerably higher Al content (SEM/EDS, TEM/EDS) has been found in both non-treated and annealed samples ($600^oC$/5 minutes). Only the monoclinic $FeAl_3Zn_x$ phase however was revealed in the annealed sample (TEM/electron diffraction) remaining uncertain the presence of the orthorhombic $Fe_2Al_5Zn_x$ phase, reported by several authors.

*Keywords*: zinc coating, galfan, heat treatment, interface, ternary Fe-Al-Zn compounds

Przeprowadzono badania mikrostruktury pokryć cynkowych typu *Galfan* na podłożu stalowym w obszarze przejścia warstwa – podłoże. Materiałem do badań były dostępne na rynku próbki pokrywanych blach otrzymanych metodą zanurzeniową w kąpieli zawierającej 5-7% wagowych Al. Zastosowanie szeregu metod analitycznych (SEM/EDS, XRD, TEM/AEM/EDS/ED) pozwoliło na ujawnienie dwufazowej struktury w próbkach przed obróbką cieplną: bogata w cynk faza eta ($\eta$) jest otoczona mieszaniną eutektyczną składającą się z płytek beta ($\beta$) aluminium oraz fazy eta ($\eta$) cynku. Warstwa przejściowa pomiędzy pokryciem cynkowym i podłożem stalowym charakteryzująca się wyższą zawartością aluminium została znaleziona (SEM/EDS, TEM/EDS) zarówno w próbkach przed obróbką cieplną, jak i w próbkach przeżarzanych ($600°C$/5 minut). Jednak wbrew doniesieniom kilku autorów nie potwierdzono obecności rombowej fazy $Fe_2Al_5Zn_x$, a stwierdzono obecność jedynie jednoskośnej fazy $FeAl_3Zn_x$ (TEM/SAED) i to tylko w próbkach przeżarzonych.

### 1. Introduction

One of the main successful application fields of the *Galfan* coatings, considered as an anticorrosion protection, is an automotive industry. But the problem of the coatings long term stability seems to be still unresolved. Introduction of certain aluminium amount into the classic zinc bath plays a dual role. It is believed the *Galfan* coatings prevent formation of the brittle binary Fe-Zn intermetallic compounds at the zinc coating/steel substrate interface. Instead of the latter the ternary Fe-Al-Zn intermetallics of lower brittleness arise in the transition layer [1]. Their secondary role is to block at least partially the Zn diffusion into substrate and the Fe diffusion toward the zinc coating. From this point of view the microstructure and composition of the interface between the zinc coating and steel substrate seems to be essential. In practice for the *Galfan* coatings 5-7wt.% aluminium is added to the zinc bath (this composition is close to the eutectic point of the Zn-Al equilibrium phase diagram). Several papers however (for instance [2-3]) report the intermetallic $Fe_2Al_5Zn_x$ phase growth between the zinc coating and the steel substrate (as a modification of the orthorhombic $Fe_2Al_5$ [4]) even for lower Al contents (above 0.15 wt.%). Other sources suggest the interface layer is either a mixture of several binary and ternary intermetallics ($Fe_2Al_5Zn_x$/$FeZn_7$/$FeZn_{13}$) [5-6] or it has a bilayered structure $Fe_2Al_5Zn_x$/$FeAl_3Zn_x$, with the outer part next to the eutectic alloy coating being $FeAl_3Zn_x$ [7]. The intermediate layer thickness for coatings with lower Al content was estimated for 200-250 nm [3] whereas for

\*   SILESIAN UNIVERSITY OF TECHNOLOGY, DEPARTMENT OF MATERIALS SCIENCE, 40-019 KATOWICE, 8 KRASINSKIEGO STR., POLAND

\*\*   COGNOR SA., STALOWA 1, 40-610 KATOWICE, POLAND

\*\*\*   POLISH ACADEMY OF SCIENCES, INSTITUTE OF METALLURGY AND MATERIALS SCIENCE, 30-059 KRAKÓW, 25 REYMONTA STR., POLAND

\*\*\*\*   UNIVERSITY OF SILESIA, INSTITUTE OF MATERIAL SCIENCE, 40-007 KATOWICE, 12 BANKOWA STR., POLAND

the *Galfan* coatings the thickness is higher (500 nm or more [8-10, 13]). The thin film (up to 500 nm) of the ternary Fe-Al-Zn compound(s) should block zinc diffusion toward the steel substrate and iron diffusion toward the zinc coating. Moreover, the interface structure should be stable within relatively wide range of temperatures. It can be interesting to quote some figures concerning zinc solubility in the Fe-Al intermetallics. They vary from 21 wt.% [7] to 22.87 wt.% [11] for the orthorhombic $Fe_2Al_5$ phase and achieve 13.92 wt.% for the monoclinic $FeAl_3$ ($Fe_4Al_{13}$) phase [12]. It could be interesting to illustrate a microstructure evolution of the *Galfan* coating subjected to the heat treatment in air (600°C/5 min.) then cooled.

## 2. Experimental techniques

The subject of examination were samples of commercially available *Galfan* coating containing 5-7wt.% of Al, deposited by hot dipping (temperature of bath 450°C) on the low carbon steel substrate. Several techniques were employed in order to study the microstructure of the coating cross-section after annealing, its composition and crystallography: scanning electron microscopy (SEM – HITACHI S-4200), energy dispersive X-ray spectroscopy (EDS – NORAN Voyager3500), X-ray diffraction (XRD – JEOL JDX-7S & PHILIPS X-PERT), high resolution transmission electron microscopy (HRTEM – JEOL JEM3010) combined with

electron diffraction (ED), analytical electron microscopy and scanning transmission microscopy (AEM/STEM - PHILIPS CM20 TWIN) combined with energy dispersive X-ray spectroscopy (EDS – EDAX Phoenix) and electron diffraction (ED). The specific software (the EL-DYF code) has been utilized in order to simulate the electron diffraction patterns of selected binary intermetallics of known crystal structure.

## 3. Results and discussion

### 3.1. SEM/EDS examination

SEM examination (HITACHI S-4200) of the *Galfan* coating samples (polished and etched cross-section) revealed its expected microstructure: Zn-rich pre-eutectoid $\eta$ phase grains were surrounded by lamellar eutectics of $\beta$-Al and $\eta$-Zn (Fig. 1). The transition layer between the alloy coating and steel substrate of the thickness below 1 $\mu$m is clearly visible in Figures 1b, 2a, 2b. The average composition of the *Galfan* coating determined by the EDS technique (Noran Voyager 3500) was following: 7.13±0.14 wt.% Al, 2.93±0.24 wt.% Fe, 89.94±0.70 wt.% Zn (PROZA and ZAF corrections). X-ray line scans of aluminium content indicate its distinct growth in the intermediate layer for both non-treated and annealed samples (Fig. 2).
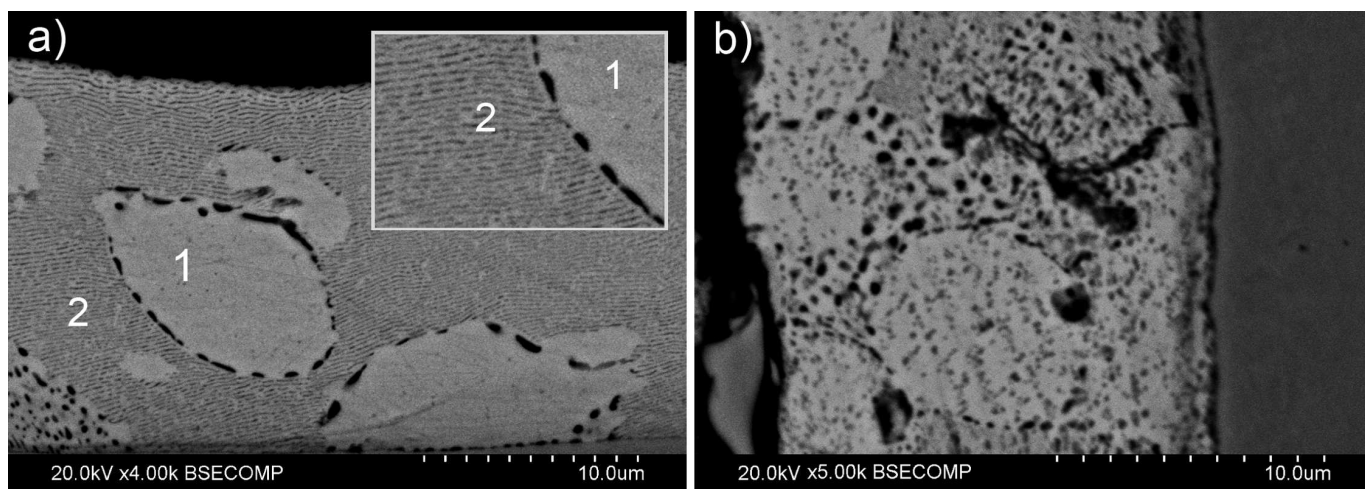


Fig. 1. SEM (BSE) micrograph of the *Galfan* coating microstructure for non-treated (a) and annealed (b) samples. (1) Zn-rich $\eta$ phase, (2) eutectics: Al-rich $\beta$ phase (lamellae) $+\eta$
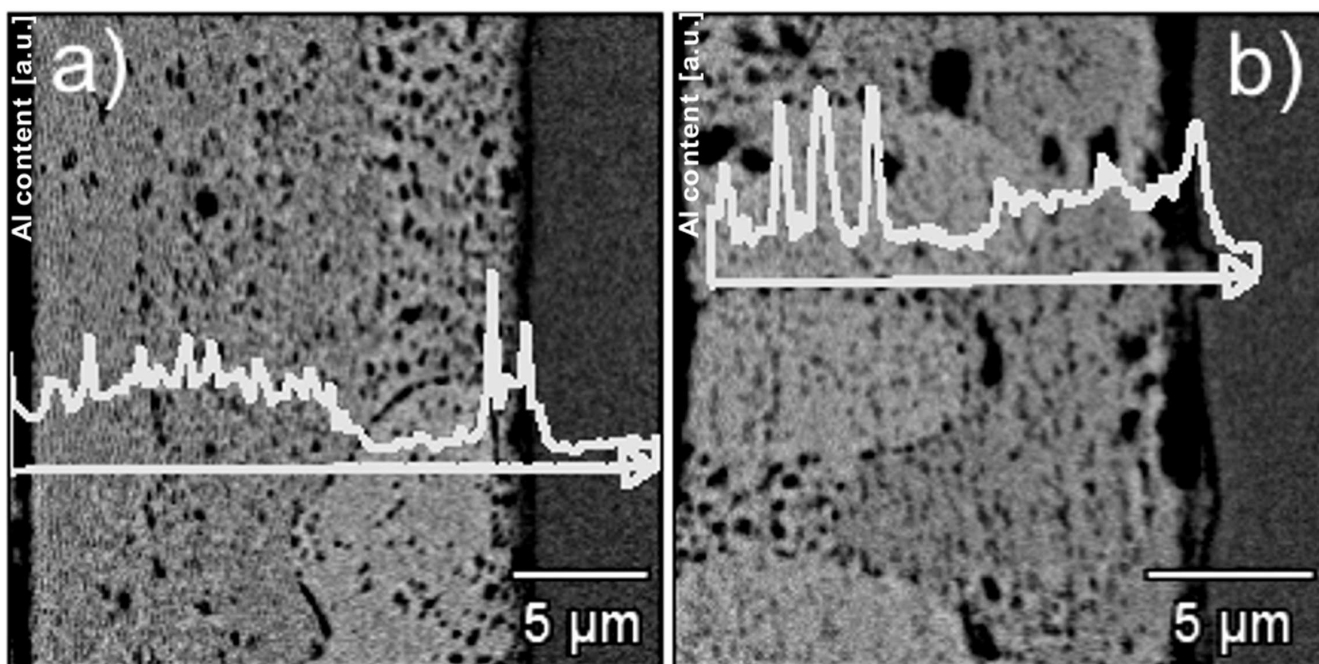
Fig. 2. X-ray aluminium line-scan at the cross-section of the *Galfan* coating for non-treated (a) and annealed (b) samples. Distinct growth of Al content at the coating/substrate interface is clearly seen
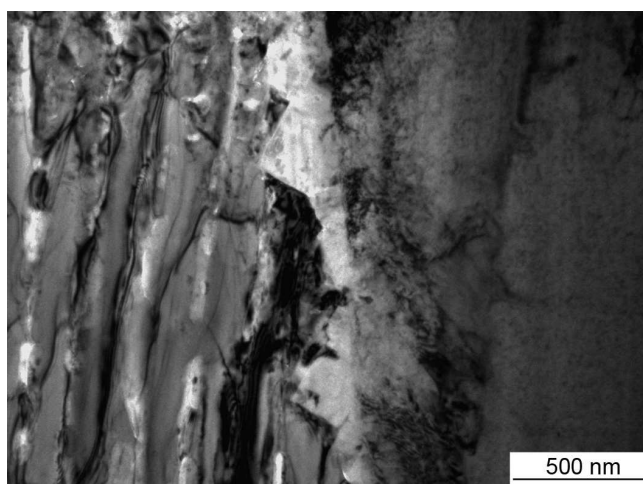


Fig. 3. Transition layer morphology in the *Galfan* coating after annealing (TEM bright field image). Visible pyramidal crystals at the coating/substrate interface

### 3.2. AEM/STEM/EDS measurements

Similar results have been achieved by an analytical electron microscopy/scanning transmission microscopy techniques (PHILIPS CM20 TWIN) combined with X-ray analysis (EDAX Phoenix). Thin foils prepared by a focused ion beam (FIB) technique (FEI Quanta 200 3D DUAL Beam) were examined with respect to their morphology and X-ray elemental distribution. Figures 3 (TEM bright field image), 4a and 4c (STEM Z-contrast, HAADF – high-angle annular dark field image) demonstrate the coating/substrate interface as a row of pyramidal crystals containing mainly aluminium and iron (see corresponding X-ray mappings in Figures 4d, 4f). Moreover, those mappings suggest two different compositions of Al-Fe compounds.
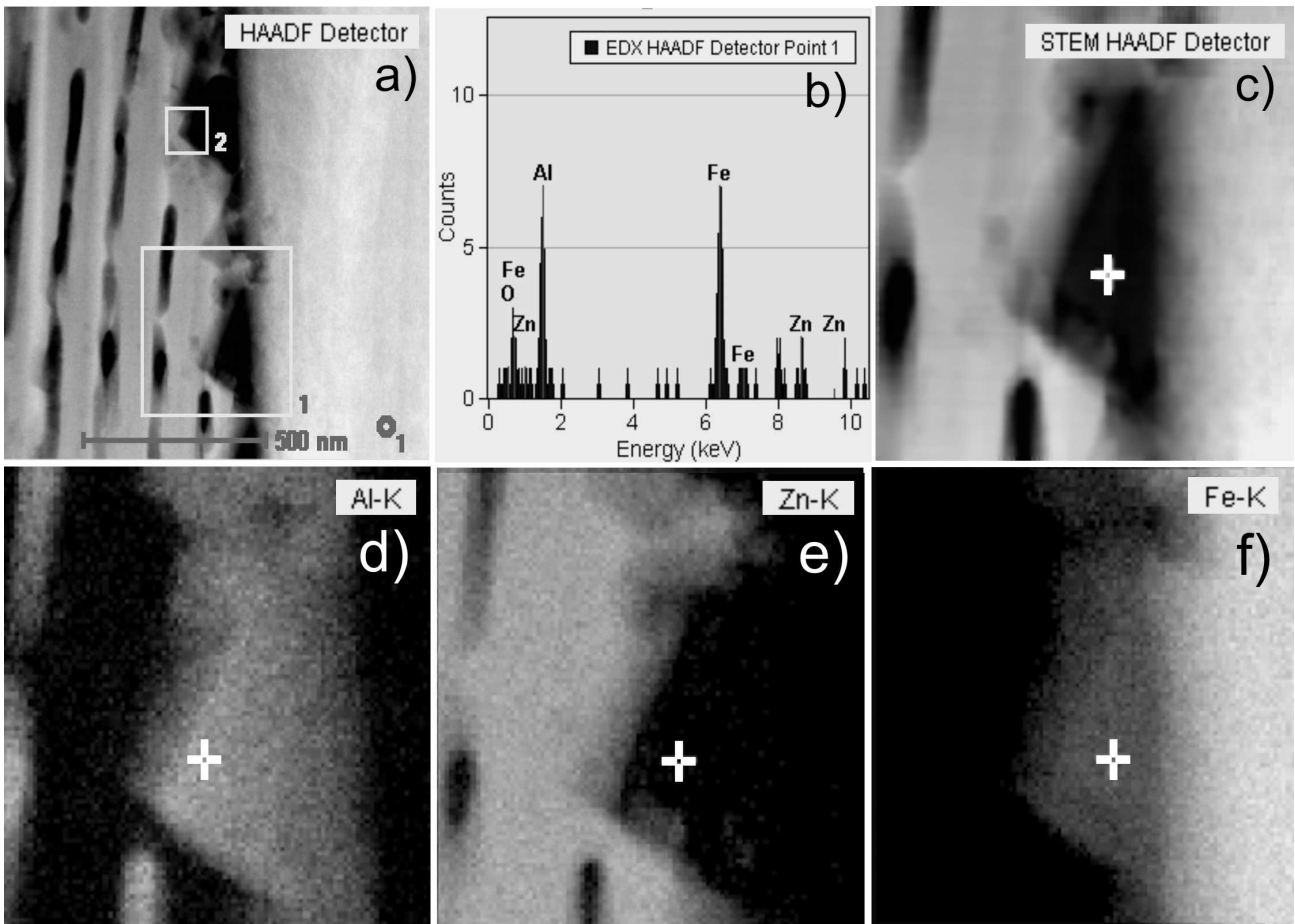
Fig. 4. Morphology of the transition layer (STEM/HAADF) in the G*alfan* coating sample after annealing (a, c), EDS X-ray spectra (b) of the pyramidal crystal (c) and corresponding Al, Zn, Fe X-ray mappings (d, e, f)

## 3.3. XRD studies

In the next stage the XRD examination of the *Galfan* coating surface after 4-step gradual grinding should expose the crystal structure of the zinc eutectic alloy, of the steel substrate and of the transition layer. X-ray diffraction patterns obtained with use of two independent instruments (JEOL JDX-7S – Cu K$\alpha_1$ radiation, Philips X-PERT – Cu K$\alpha_1$ radiation) for non-treated and annealed samples (Figures 5a and 5b respectively) show however only the presence of an eutectic zinc alloy and a steel substrate but neither the orthorhombic Fe$_2$Al$_5$Zn$_x$ nor the monoclinic FeAl$_3$Zn$_x$ (Fe$_4$Al$_{13}$Zn$_x$) have been revealed (see the respective reference patterns in Figure 5c simulated upon the data from references [4] and [12]). Since the transition layer thickness is low (below 1 $\mu$m) and consequently its volume is much lower than the alloy coating volume, X-ray diffraction peaks corresponding to the interface components should have low intensities. Additionally some interesting peaks (for instance the Fe$_2$Al$_5$ reference peak at 43.95° and the FeAl$_3$ reference peak at 43.15°) can overlap with the $\alpha$-Fe peak (110), $\beta$-Al peak (200) or $\eta$-Zn peak (101).

From the other hand potential strong reference peaks at 22.5°, 23.2°, 25.13°, 26.7°, 47.5° and 49.3° (Fig. 5c) are not visible. In the light of achieved XRD results the presence of Fe$_2$Al$_5$Zn$_x$ and FeAl$_3$Zn$_x$ (Fe$_4$Al$_{13}$Zn$_x$) intermetallic compounds in the transition layer can not be confirmed.
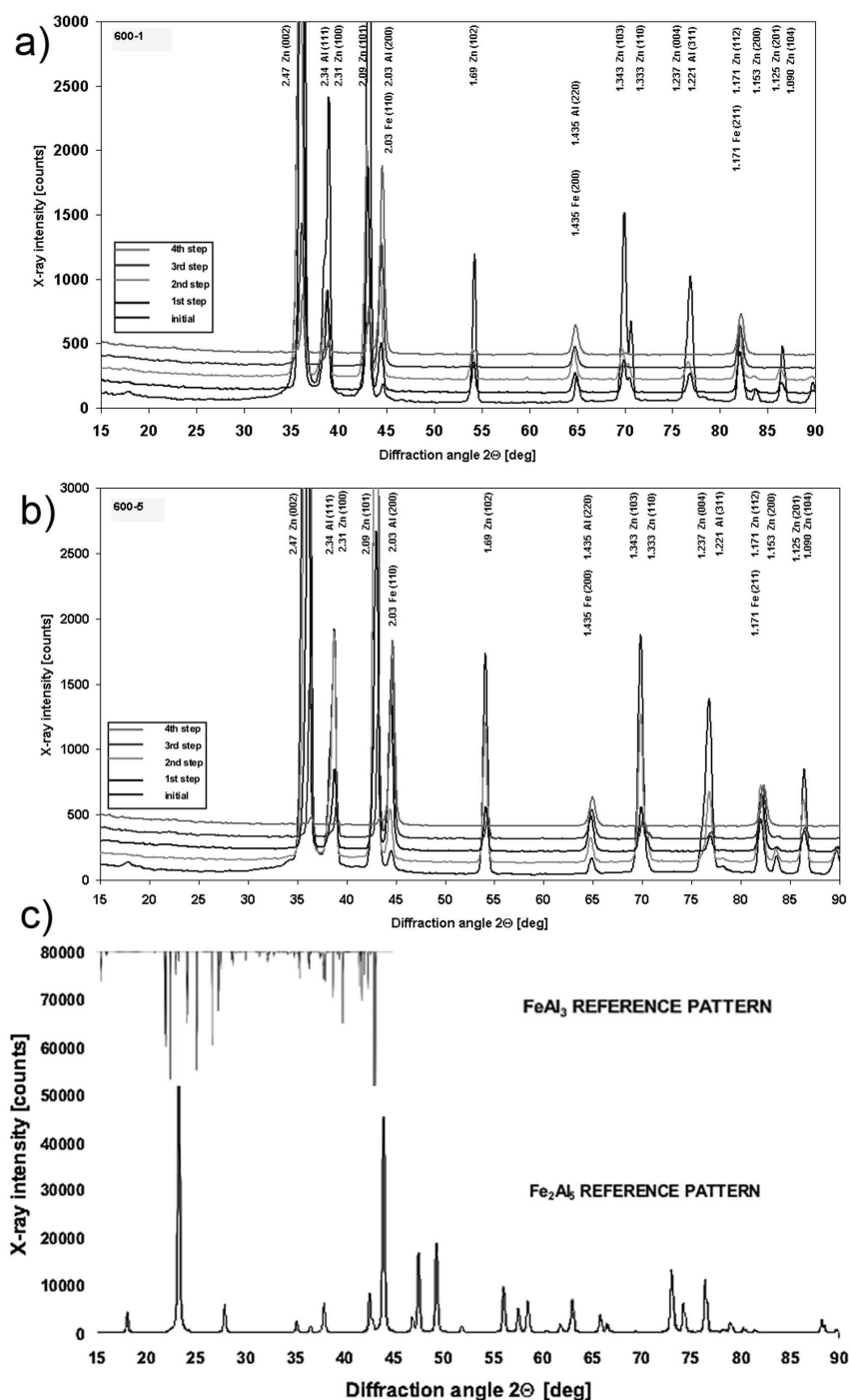
Fig. 5. X-ray diffraction patterns of the *Galfan* coating surface after 4-step gradual grinding for non-treated sample (a) and annealed (600°C/5 min.) sample (b). All diffraction peaks correspond either to the eutectic zinc alloy or to the steel substrate. The reference patterns (c) corresponding to the orthorhombic $Fe_2Al_5$ and the monoclinic $FeAl_3$ phases respectively have been simulated upon data from the references [4] and [12] respectively

### 3.4. TEM/AEM electron diffraction studies

In order to find definite answer about presence or absence of the searched intermetallic compounds at the zinc alloy/steel substrate interface a transmission electron microscopy and an electron diffraction techniques (TEM/SAED – selected area electron diffraction) were employed on thin foils at the transition layer cross-section, prepared by the FIB technique (two independent instruments PHILIPS CM20 TWIN and JEOL JEM-3010). Additionally the ELDYF software was applied in order to simulate the reference electron diffraction patterns for the orthorhombic $Fe_2Al_5$ and the monoclinic $FeAl_3$ ($Fe_4Al_{13}$) at various zone axes. The atom coordinates in the unit cell were taken from the

references [4] and [12] for the orthorhombic $Fe_2Al_5$ and the monoclinic $FeAl_3$ ($Fe_4Al_{13}$) respectively. Results of the observations (bright and dark field images) and respective electron diffraction patterns (SAED) together with corresponding ED simulations at various zone axes are shown in Figures 6, 7, 8. The detailed analysis of several experimental SAED patterns allowed to conclude that only the monoclinic $FeAl_3$ ($Fe_4Al_{13}$) simulated patterns match the experimental diffraction patterns (see Figures 6c, 6d, 7b, 7c and 8b, 8c). The comparison of the orthorhombic $Fe_2Al_5$ simulations to several measured SAED patterns gave the negative result.
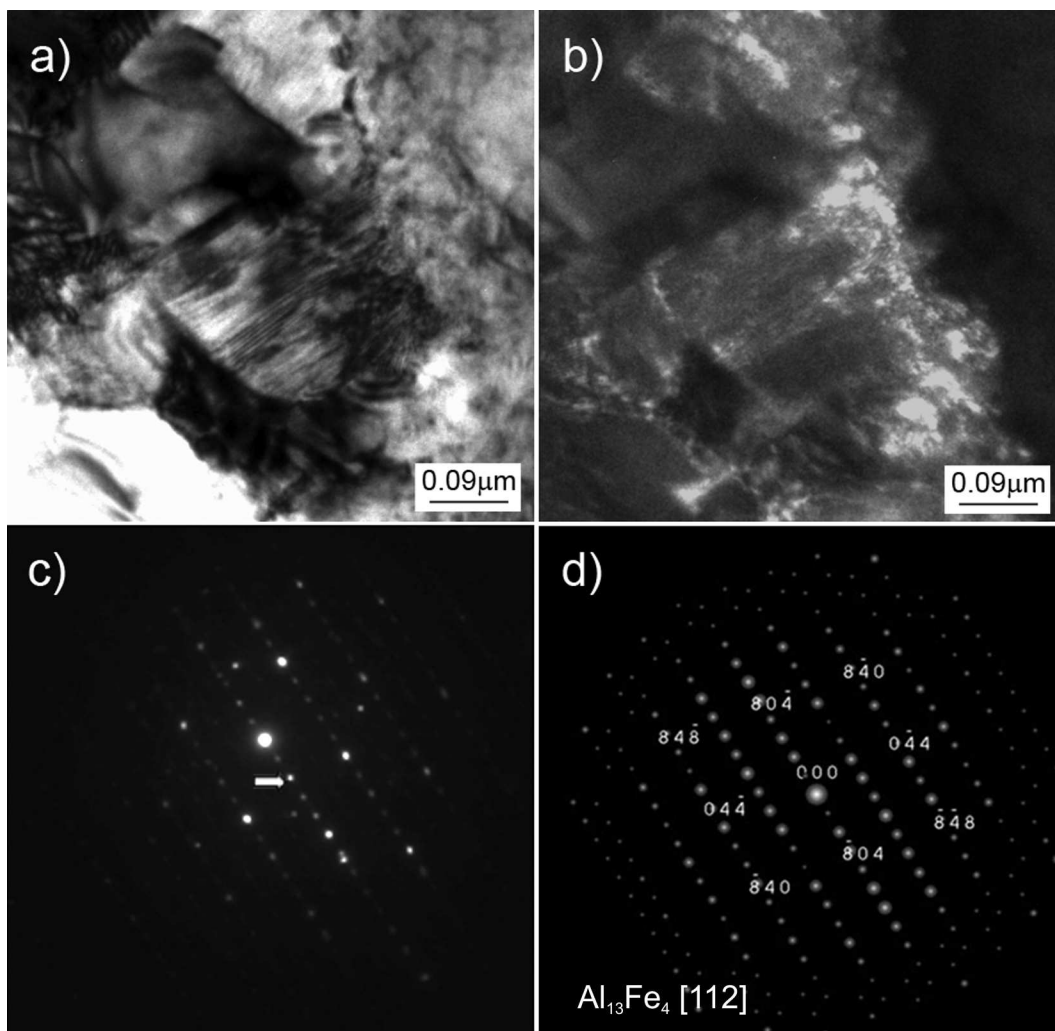


Fig. 6. TEM micrograph of the coating/substrate area. Bright field image (a), dark field image (b) at the ED reflex indicated by white arrow (c) and corresponding indexed simulation of the $FeAl_3$ ($Fe_4Al_{13}$) diffraction (d). Atoms unit cell coordinates taken from the reference [12]
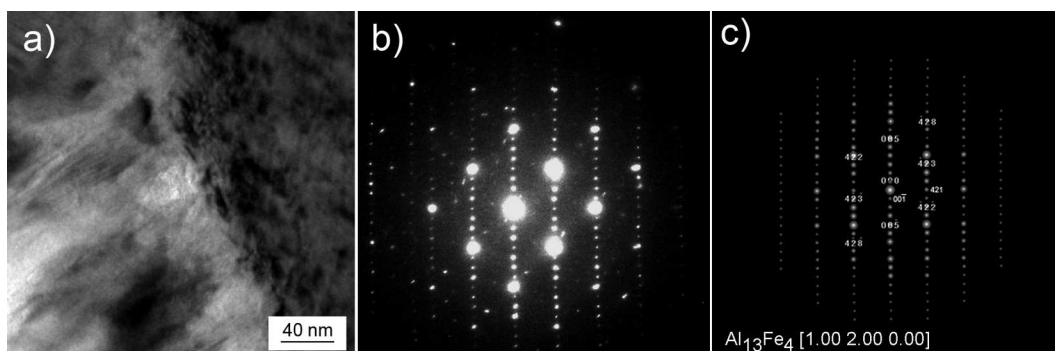


Fig. 7. TEM micrograph of the coating/substrate area. Bright field image (a), the measured electron diffraction pattern (b) and corresponding indexed simulation of the $FeAl_3$ ($Fe_4Al_{13}$) electron diffraction at the zone axis [041] (c). Atoms unit cell coordinates taken from the reference [12]
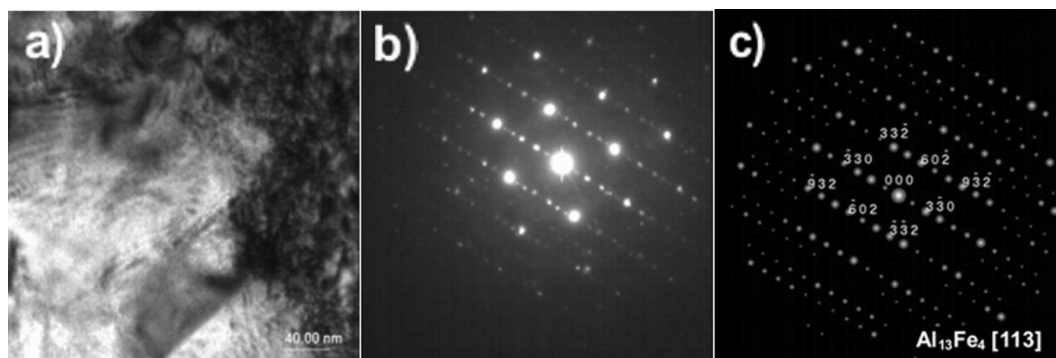
Fig. 8. TEM micrograph of the coating/substrate area. Bright field image (a), the measured electron diffraction pattern (b) and corresponding indexed simulation of the FeAl₃ (Fe₄Al₁₃) electron diffraction at the zone axis [113] (c). Atoms unit cell coordinates taken from the reference [12]

## 4. Summary

The commercially available *Galfan* coating samples subject to heat treatment (600°C/5 min. in air) appeared to hold stable microstructure and thickness. The zinc coating/steel substrate interface (transition layer) satisfies its main role and prevents formation of brittle binary Fe-Zn compounds. From several binary and ternary compounds reported by other authors only the monoclinic $FeAl_3Zn_x$ ($Fe_4Al_{13}Zn_x$) has been confirmed by TEM/SAED (electron diffraction) technique in the transition layer. Disappointing results of our XRD examination (searching of any of ternary Fe-Al-Zn intermetallics at the coating/substrate interface) can be produced however as a consequence of too low volume of the layer in comparison to the total coating volume.

### REFERENCES

[1] A.R. M a r d e r, The metallurgy of zinc-coated steel, Progress of Materials Science **45**, 191-271 (2000).

[2] M. G u t t m a n n, Y. L e p r e t r e, A. A u b r y, M-J. R o c h e, T. M o r e a u, P. D r i l l e t, J.M. M a t a i g n e, H. B a u d i n, Mechanism of the galvanizing reaction. Influence of Ti and P contents in steel and of its surface microstructure after annealing, in: GALVATECH '95, Chicago, Iron and Steel Society, 295 (1995).

[3] N.Y. T a n g, Modeling of enrichment in galvanized coatings, Met Mater Trans. **26A**, 1669 (1995).

[4] U. B u r k h a r d t, J. G r i n, M. E l l n e r, K. P e t e r s, Structure refinement of the iron-aluminium phase with the approximate composition Fe₂Al₅, Acta Cryst. **B50**, 313-316 (1994).

[5] K. I c h i y a m a, J. K o b a y a s h i, S. S u g i m o t o, Proceedings of 14th International Hot Dip Galvanization Conference, Munich, Zinc Development Association 9/1 (1985).

[6] S.J. M a k i m a t t i l a, On the production possibilities of a deep drawing quality Zn-5% Al coated steel sheet, Scan J Metall **15**, 224 (1986).

[7] Z.W. C h e n, J.T. G r e g o r y, R.M. S h a r p, Intermetallic phases formed during hot dipping of low carbon steel in a Zn-5%Al melt at 450°C, Met Trans. **23A**, 2393 (1992).

[8] P.G. C a c e r e s, C.A. H o t h a m, J.A. S p i t t l e, R.D. J o n e s, Mechanisms of formation and growth of inter-metallic layers during hot dipping of iron in Zn-3Al and Zn-6Al baths, Mater Sci Technol **2**, 871 (1986).

[9] J. P e l e r i n, J.P. S e r v a i s, D. C o u t s o u r a d i s, D.C. H e r r s c h a f t, S.F. R a d k e, Proceedings of 13ᵗʰ International Hot Dip Galvanization Conference, London, Zinc Development Association, 49/I (1982).

[10] J. K l i ś, A. T o m a s z e w s k a, E. A u g u s t y n, J. G r z o n k a, G. M o s k a l, H. W o ź n i c a, M. Ż e l e c h o w e r, Mikrostruktura i skład chemiczny powłok typu *Galfan* po obróbce cieplnej, Inżynieria Materiałowa (Materials Science), 3, 174-181 (in Polish with abstract in English) (2009).

[11] M. U r e d n i c e k, J.S. K i r k a l d y, Mechanism of iron attack inhibition arising from additions of aluminum to liquid Zn(Fe) during galvanizing, Zeitschrift fur Metallkunde **64**, 649 (1987).

[12] J. G r i n, U. B u r k h a r d t, M. E l l n e r, K. P e t e r s, Refinement of the Fe₄Al₁₃ structure and its relationship to the quasihomological homeotypical structures, Zeitschrift fur Kristallogr. **209**, 479-487 (1994).

[13] J. W e s o ł o w s k i, W. G ł u c h o w s k i, L. C i u r a, New lead free zinc alloy for unit mode hot – dip galvanising of steel products, Archives of Metallurgy and Materials **51**, 2, 283 (2006).